

Direct Measurements of Charmed D Meson Hadronic Branching Fractions*

R.M. Baltrusaitis, J.J. Becker, G.T. Blaylock, J.S. Brown, K.O. Bunnell,
T.H. Burnett, R.E. Cassell, D. Coffman, V. Cook, D.H. Coward, S. Dado, D.E. Dorfan,
G.P. Dubois, A.L. Duncan, K.F. Einsweiler, B.I. Eisenstein, R. Fabrizio, G. Gladding, F. Grancagnolo,
R.P. Hamilton, J. Hauser, C.A. Heusch, D.G. Hitlin, L. Köpke, W.S. Lockman, U. Mallik,
P.M. Mockett, R.F. Mozley, A. Nappi, A. Odian, R. Partridge, J. Perrier, S.A. Plaetzer,
J.D. Richman, J. Roehrig, J.J. Russell, H.F.W. Sadrozinski, M. Scarlatella, T.L. Schalk,
R.H. Schindler, A. Seiden, C. Simopoulos, J.C. Sleeman, A.L. Spadafora, I.E. Stockdale,
J.J. Thaler, B. Tripsas, W. Toki, F. Villa, A. Wattenberg, A.J. Weinstein, N. Wermes,
H.J. Willutzki, D. Wisinski, W.J. Wisniewski, G. Wolf

The MARK III Collaboration

California Institute of Technology, Pasadena, CA 91125
University of California at Santa Cruz, Santa Cruz, CA 95064
University of Illinois at Urbana-Champaign, Urbana, IL 61801
Stanford Linear Accelerator Center, Stanford, CA 94305
University of Washington, Seattle, WA 98195

Abstract

A new technique is applied to data collected at the $\psi(3770)$ resonance to derive charmed D meson branching fractions without relying on the measurement of D production cross sections. Measurements are presented for three decay modes of the D^0 ($K^-\pi^+$, $K^-\pi^-\pi^+\pi^+$ and $K^-\pi^+\pi^0$) and four decay modes of the D^+ ($K^-\pi^+\pi^+$, $K^-\pi^+\pi^+\pi^0$, $K_s^0\pi^+$ and $K_s^0\pi^+\pi^0$). The resulting branching fractions are significantly larger than previous measurements.

Submitted to *Physical Review Letters*

* Work supported in part by the National Science Foundation, and by the Department of Energy under Contracts DE-AC03-76SF00515, DE-AC02-76ER01195, DE-AC03-81ER40050, and DE-AM03-76SF00034.

The exclusive production of $D^0\bar{D}^0$ and D^+D^- pairs at the $\psi(3770)$ resonance provides a unique opportunity to measure charmed D meson branching fractions directly. Previous measurements at this resonance of D hadronic branching fractions¹⁻³ have relied on a determination of the charm production cross section (σ_D) to normalize observed D meson production rates. However, the kinematics of $D\bar{D}$ pair production at the $\psi(3770)$ makes it possible to measure D branching fractions independent of σ_D . The results obtained by this method differ significantly from earlier results.

The data were collected with the Mark III detector⁴ at the e^+e^- storage ring SPEAR at an average energy of $\sqrt{s} = 3.768$ GeV. We assume that events containing charmed D mesons arise solely from $D\bar{D}$ production, so that the detection of a single D in an event implies that the recoiling system is a monochromatic \bar{D} .⁵ The data are searched for events containing either one or two reconstructed D mesons. For this analysis, three D^0 decay channels ($K^-\pi^+$, $K^-\pi^-\pi^+\pi^+$ and $K^-\pi^+\pi^0$) and four D^+ decay channels ($K^-\pi^+\pi^+$, $K^-\pi^+\pi^+\pi^0$, $K_s^0\pi^+$ and $K_s^0\pi^+\pi^0$) are considered. By comparing the number of times a single D (or \bar{D}) is reconstructed (*single-tags*) with the number of fully reconstructed $D\bar{D}$ events (*double-tags*), the individual D meson branching fractions can be derived independently of σ_D .

Single-tag reconstruction proceeds as follows. Charged particles are required to satisfy $|\cos\theta| < 0.85$ (where θ is the polar angle with respect to the beam) to insure reliable drift chamber measurements. A charged particle which enters the time-of-flight (TOF) system ($|\cos\theta| < 0.75$) is identified as either a π or K, according to which predicted time is closer to the measured time. Unidentified tracks are assumed to be pions. Showers with energies greater than 0.050 GeV

are used as photon candidates. Neutral kaons are detected through the decay $K_s^0 \rightarrow \pi^+\pi^-$, where the $\pi^+\pi^-$ invariant mass is required to lie within $0.0156 \text{ GeV}/c^2$ of the K_s^0 mass. Appropriate combinations of charged tracks and photons are formed for the three D^0 and four D^+ decay modes under study. To improve mass resolution and further reduce backgrounds, the energy of each D candidate is constrained to the beam energy (E_b). The small spread in E_b ($\sigma_{E_b} = 0.0015 \text{ GeV}$) and the low D momenta ($0.245 \text{ GeV}/c$ for D^+ and $0.285 \text{ GeV}/c$ for D^0) produce a mass resolution of $\sigma_M \sim 0.003 \text{ GeV}/c^2$. Modes containing a π^0 are fit to the two constraints of beam energy and π^0 mass, and fits with $\chi^2 > 6$ are removed. The resulting mass distributions for the single-tag modes are shown in Figure 1. In each case, a flat background determined from the control region 1.83 to $1.85 \text{ GeV}/c^2$ is subtracted and the number of single-tags is counted over a region dependent on the specific decay mode.

Double-tags are subject to additional constraints. Events are fit to the hypothesis:

$$e^+e^- \rightarrow X\bar{X} \rightarrow \text{final state}$$

where $M_X = M_{\bar{X}}$. Energy-momentum conservation for $D\bar{D}$ production provides six constraints (with an additional constraint for each π^0 or K_s^0), all but one of which are used in kinematic fitting (*i.e.* M_X is not fixed at M_D). The improved background rejection provided by the constrained fit permits loosening of the particle identification cuts, thereby improving detection efficiency. Charged tracks are assigned as either π 's or K's (or both), requiring only consistency with the TOF times and the dE/dx pulse height measurements.⁶ When no information is present, or the information is inconclusive, both hypotheses are

considered. The resulting distributions of M_X are shown in Figure 2 for six $D^0\bar{D}^0$ and four D^+D^- decay modes. A constant background is determined from the control region 1.83 to 1.85 GeV/c^2 . Events within $\pm 0.008 \text{ GeV}/c^2$ of the D mass constitute the signal.

To determine the individual branching fractions (B_i) and the number of produced $D\bar{D}$ pairs (N), the corrected number of single-tags (S_i) and double-tags (D_{ij}) are employed in a χ^2 minimization fit, using the following expressions:

$$\begin{aligned}
 S_i &= 2NB_i\epsilon_i - \sum_j 2NB_iB_j\alpha_{ij}^i \\
 D_{ij} &= 2NB_iB_j\epsilon_{ij} \quad \text{if } i \neq j \\
 D_{ii} &= NB_i^2\epsilon_{ii}
 \end{aligned}$$

where ϵ_i is the efficiency for reconstructing a single-tag in the i th D decay mode, ϵ_{ij} is the efficiency for reconstructing a double-tag for $D\bar{D}$ decay modes i and j , and α_{ij}^i is the efficiency for reconstructing a single-tag of mode i while simultaneously reconstructing the entire event as a double-tag of modes i and j . The second term in the expression for S_i removes from the single-tag sample those tags which also appear in the double-tag sample. This subtraction leaves the two samples independent and eliminates the problem of directly correlated errors. The efficiencies are determined by a detailed Monte Carlo simulation of $D\bar{D}$ production and decay, including the detector response. Fits are performed separately for neutral D's and charged D's, yielding $21400^{+1600}_{-1400} \pm 1400$ produced $D^0\bar{D}^0$ events and $16000^{+2100}_{-1700} \pm 800$ produced D^+D^- events (where the first error is statistical and the second systematic). A comparison of the observed numbers of tags with the predictions from the fits is shown in Table I. The fit to neutral D's yields a χ^2 of 4.05 for 5 degrees of freedom while the fit to charged D's yields

a χ^2 of 4.79 for 3 degrees of freedom. The ratio of $D^0\overline{D}^0$ to D^+D^- production is not constrained in the fits, but the measured result ($1.34_{-0.20}^{+0.17} \pm 0.11$) agrees well with the ratio (1.36) predicted by Eichten et al.⁷ using a coupled channel model. The fitted values for the D branching fractions, summarized in Table II, are significantly larger than previous determinations. Finally, the measurements of $B(K^-\pi^+)$, $B(\overline{K}^0\pi^+)$, and $B(K^-\pi^+\pi^+)$ can be used to express our previous relative measurements of Cabbibo suppressed D decays as absolute branching fractions.⁸

The systematic errors on the fitted branching fractions arise from several sources. The uncertainties in charged particle tracking efficiency and particle identification contribute less than 2% to the uncertainty in final state efficiencies. The uncertainty in the estimated detection efficiency for π^0 's (resulting primarily from the modelling of gaps and support structures in the shower counter) is about 5% for modes containing a single π^0 . In addition, backgrounds in specific single-tag modes ($D^0 \rightarrow K^-\pi^+\pi^0$, $D^+ \rightarrow K_s^0\pi^+\pi^0$ and $D^+ \rightarrow K^-\pi^+\pi^+\pi^0$) may not be flat. In these cases, allowances for other background shapes have been included, contributing 5-16% uncertainty to the efficiencies for these decay modes. The resonance substructure in three-body and four-body final states introduces an additional uncertainty in the detection efficiencies of not more than 15%.⁹

There are several interesting consequences of these larger D branching fraction measurements. The D^0 and D^+ cross sections at the $\psi(3770)$ can be derived from the number of produced $D\overline{D}$ events together with luminosity measurements. The integrated luminosity as determined from wide angle Bhabha scattering and $\mu^+\mu^-$ events is $9558 \pm 479 \text{ nb}^{-1}$. Using this value, we obtain $\sigma_{D^0} = 4.48_{-0.29}^{+0.33} \pm 0.37 \text{ nb}$ and $\sigma_{D^+} = 3.35_{-0.36}^{+0.44} \pm 0.24 \text{ nb}$.¹⁰ These are substantially smaller

than previous values¹¹ derived from the direct measurement of $\sigma_{\psi(3770)}$.¹² To further understand this discrepancy, the cross section times branching fractions ($\sigma_D \cdot B_i$) for the seven channels studied can be derived from the unsubtracted single-tags. These results, along with previous measurements summarized in Table II, show very good agreement between experiments. It is the division by each experiment's value for σ_D which leads to the systematic difference in branching fractions.¹³ This suggests either that the discrepancies in branching fractions lie with the measurements of σ_D , or that the underlying assumption of the previous measurements, namely that the $\psi(3770)$ decays exclusively to $D\bar{D}$, is incorrect. Furthermore, our larger values of the D branching fractions reduce previous determinations of charm production cross sections and branching fractions of heavy mesons which cascade through D hadronic modes.

We gratefully acknowledge the efforts of the SPEAR staff. This work was supported in part by the U.S. National Science Foundation and the U.S. Department of Energy under Contracts No.DE-AC03-76SF00515, No.DE-AC02-76ER01195, No.DE-AC03-81ER40050, and No.DE-AM03-76SF00034.

REFERENCES

1. I. Peruzzi et al., Phys. Rev. Lett. **39**, 1301 (1977).
2. D.L. Scharre et al., Phys. Rev. Lett. **40**, 74 (1978).
3. R. H. Schindler et al., Phys. Rev. **D24**, 78 (1981).
4. For a description of the Mark III detector see D. Bernstein et al., Nucl. Instr. and Meth. **226**, 301 (1984).
5. Throughout this paper, we adopt the convention that reference to a state also implies reference to its charge conjugate. The effects of $D^0\bar{D}^0$ mixing and doubly Cabibbo suppressed decays are expected to be negligible and are ignored.
6. For TOF consistency, the measured time must match the predicted time for a π or K within four standard deviations (σ), where $\sigma \sim 190$ ps. Consistency with the dE/dx measurement implies that the truncated mean of six to twelve ionization measurements is within 3σ (4.5σ) of the predicted value on the low (high) side, where $\sigma \sim 15\%$ of the peak value. For further description of the dE/dx system see: J. Roehrig et al., Nucl. Instr. Meth. **226**, 319 (1984).
7. E. Eichten et al., Phys. Rev. **D21**, 203 (1980).
8. Using our fitted values of $B(K^-\pi^+)$, $B(\bar{K}^0\pi^+)$, and $B(K^-\pi^+\pi^+)$, the results

of R. M. Baltrusaitis et al., Phys. Rev. Lett. **55**, 150 (1985) become:

$$B(D^0 \rightarrow K^+K^-) = 0.68 \pm 0.11 \pm 0.08\%$$

$$B(D^0 \rightarrow \pi^+\pi^-) = 0.18 \pm 0.06 \pm 0.04\%$$

$$B(D^+ \rightarrow K^+\overline{K}^0) = 1.30 \pm 0.40 \pm 0.22\%$$

$$B(D^+ \rightarrow \pi^+\pi^+\pi^-) = 0.49 \pm 0.19 \pm 0.12\%$$

$$B(D^+ \rightarrow K^+K^- \pi^+)_{\text{non-res.}} = 0.68 \pm 0.31 \pm 0.11\%$$

$$B(D^+ \rightarrow \phi\pi^+) = 0.97 \pm 0.27 \pm 0.14\%$$

$$B(D^+ \rightarrow \overline{K}^{*0}K^+) = 0.56 \pm 0.25 \pm 0.13\%$$

9. The substructure of the 3-body decays, taken from R. H. Schindler, Proc. of the SLAC Summer Inst. of Particle Physics, 1985 (SLAC-PUB-3799), implies less than 5% uncertainty in the final state efficiencies. For $K^-\pi^-\pi^+\pi^+$, the results of M. Piccolo et al., Phys. Lett. **70B**, 260 (1977) have been used. Since no measurements for $K^-\pi^+\pi^+\pi^0$ have been reported, we use a phase space decay with a 15% uncertainty in reconstruction efficiency.

10. Note σ_{D^0} is defined to be twice $\sigma_{D^0\overline{D}^0}$ and σ_{D^+} is twice $\sigma_{D^+D^-}$.

11. Values of σ_{D^0} and σ_{D^+} derived from the measurements of the total hadronic cross section are $\sigma_{D^0} = 11.5 \pm 2.5$ and $\sigma_{D^+} = 9.0 \pm 2.0$ (I. Peruzzi et al., Phys. Rev. Lett. **39**, 1301 (1977)), $\sigma_{D^0} = 8.0 \pm 1.0 \pm 1.2$ and $\sigma_{D^+} = 6.0 \pm 0.7 \pm 1.0$ (R. H. Schindler et al., Phys. Ref. **D21**, 2716 (1980)), and $\sigma_{D^0} = 6.8 \pm 1.2$ and $\sigma_{D^+} = 6.0 \pm 1.1$ (H. Sadrozinski, Proc. of the XXth Int. Conf. on High Energy Physics, Madison, Wisconsin p.681 (1980)).

12. The direct measurement of $\sigma_{\psi(3770)}$ leads to predictions for σ_{D^0} and σ_{D^+} by using the ratio of D^0 to D^+ production predicted by p-wave phase space and assuming that the $\psi(3770)$ decays exclusively to $D\bar{D}$.
13. Similar discrepancies have been noted by previous experiments, with lower statistical significance. Rafe H. Schindler, SLAC-Report-219 p. 160 (1979); M. Aguilar-Benitez et al., Phys. Lett. **135**, 237 (1984); M. Aguilar-Benitez et al., Phys. Lett. **146B**, 266 (1984).

TABLE CAPTIONS

1. Comparison of single and double-tag measurements and fit results. Reference to a state also implies reference to its charge conjugate. The overlaps with double-tags have been subtracted from the single-tags.
2. Comparison of D production cross sections (nb) at the $\psi(3770)$, cross section times branching fractions (nb), and derived branching fractions (%).

Table I-a

D ⁰ Tags	K ⁻ π ⁺	K ⁻ π ⁺ π ⁰	K ⁻ π ⁺ π ⁻ π ⁺
K ⁺ π ⁻	26 ± 6	95 ± 11	50 ± 8
(fit)	29	91	59
K ⁺ π ⁻ π ⁰		69 ± 17	105 ± 13
(fit)		70	89
K ⁺ π ⁻ π ⁺ π ⁻			22 ± 6
(fit)			23
single tags	930 ± 37	930 ± 64	992 ± 55
(fit)	916	978	985

Table I-b

D ⁺ Tags	K ⁻ π ⁺ π ⁺	K ⁻ π ⁺ π ⁺ π ⁰	K _s ⁰ π ⁺	K _s ⁰ π ⁺ π ⁰
K ⁺ π ⁻ π ⁻	39 ± 7	35 ± 9	13 ± 4	18 ± 6
(fit)	45	20	12	16
single tags	1164 ± 42	175 ± 43	161 ± 14	159 ± 32
(fit)	1155	210	162	165

Table II

Decay Mode	LGW ^{1,2}	Mark II ³	This Experiment
σ_{D^0}	11.5 ± 2.5	$8.0 \pm 1.0 \pm 1.2$	$4.48^{+.33}_{-.29} \pm .37$
$\sigma B(K^- \pi^+)$	0.25 ± 0.05	0.24 ± 0.02	$0.248 \pm 0.009 \pm 0.014$
$B(K^- \pi^+)$	2.2 ± 0.6	3.0 ± 0.6	$5.6 \pm 0.4 \pm 0.3$
$\sigma B(K^- \pi^- \pi^+ \pi^+)$	0.36 ± 0.10	0.68 ± 0.11	$0.525 \pm 0.026 \pm 0.054$
$B(K^- \pi^- \pi^+ \pi^+)$	3.2 ± 1.1	8.5 ± 2.1	$11.8 \pm 0.9 \pm 1.1$
$\sigma B(K^- \pi^+ \pi^0)$	1.4 ± 0.6	0.68 ± 0.23	$0.759 \pm 0.044 \pm 0.083$
$B(K^- \pi^+ \pi^0)$	12 ± 6	8.5 ± 3.2	$17.5 \pm 1.3 \pm 1.3$
σ_{D^+}	9.0 ± 2.0	$6.0 \pm 0.7 \pm 1.0$	$3.35^{+.44}_{-.36} \pm .24$
$\sigma B(K^- \pi^+ \pi^+)$	0.36 ± 0.06	0.38 ± 0.05	$0.388 \pm 0.013 \pm 0.029$
$B(K^- \pi^+ \pi^+)$	3.9 ± 1.0	6.3 ± 1.5	$11.6 \pm 1.4 \pm 0.7$
$\sigma B(K^- \pi^+ \pi^+ \pi^0)$			$0.177 \pm 0.042 \pm 0.042$
$B(K^- \pi^+ \pi^+ \pi^0)$			$6.3^{+1.4}_{-1.3} \pm 1.2$
$\sigma B(\bar{K}^0 \pi^+)$	0.14 ± 0.05	0.14 ± 0.03	$0.135 \pm 0.012 \pm 0.010$
$B(\bar{K}^0 \pi^+)$	1.5 ± 0.6	2.3 ± 0.7	$4.1 \pm 0.6 \pm 0.3$
$\sigma B(\bar{K}^0 \pi^+ \pi^0)$		0.78 ± 0.48	$0.417 \pm 0.081 \pm 0.075$
$B(\bar{K}^0 \pi^+ \pi^0)$		12.9 ± 8.4	$12.9^{+2.7}_{-2.6} \pm 2.1$

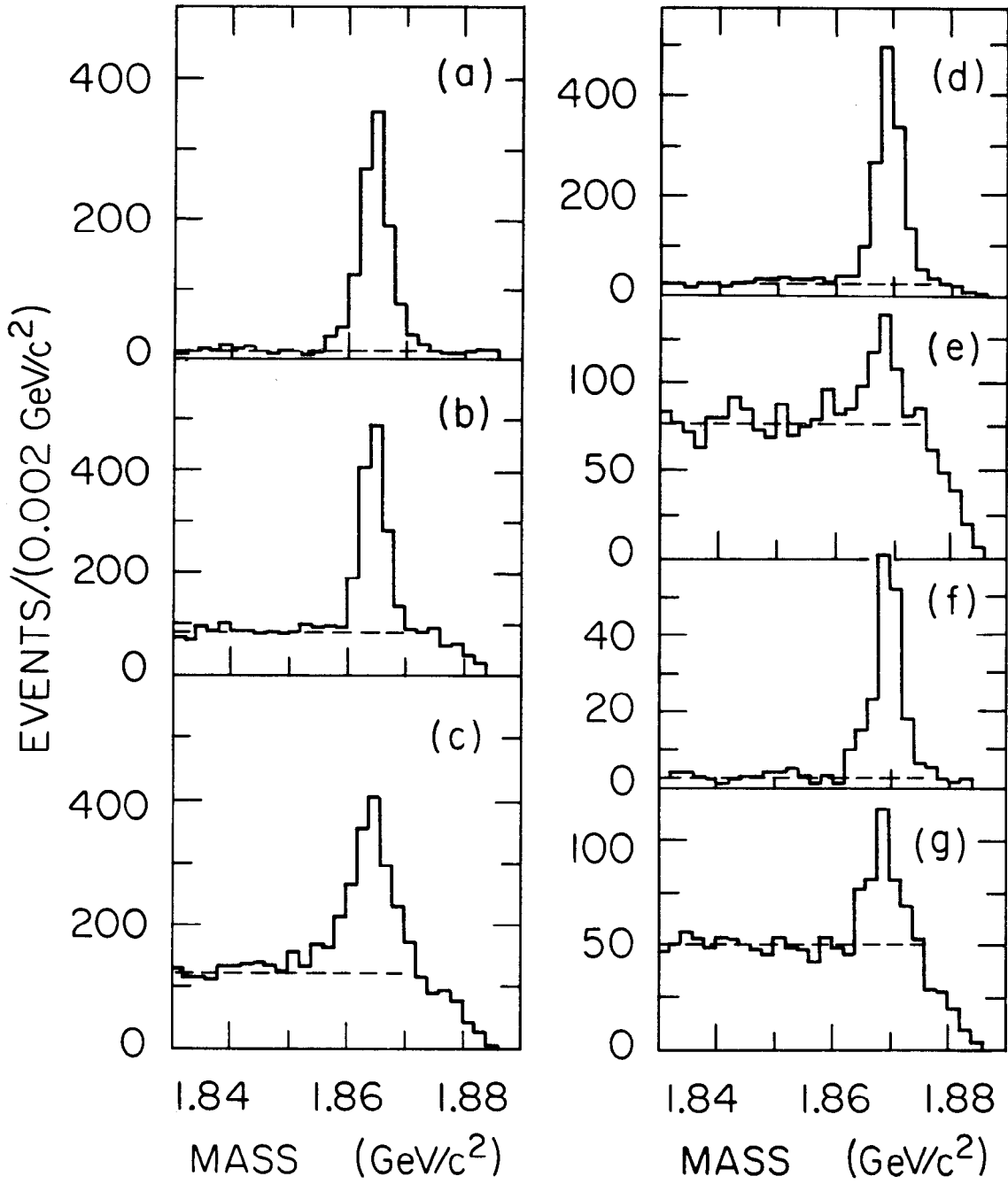
FIGURE CAPTIONS

1. Beam constrained mass for single-tags:

(a) $D^0 \rightarrow K^-\pi^+$, (b) $D^0 \rightarrow K^-\pi^-\pi^+\pi^+$, (c) $D^0 \rightarrow K^-\pi^+\pi^0$, (d) $D^+ \rightarrow K^-\pi^+\pi^+$, (e) $D^+ \rightarrow K^-\pi^+\pi^+\pi^0$, (f) $D^+ \rightarrow K_s^0\pi^+$, (g) $D^+ \rightarrow K_s^0\pi^+\pi^0$.

2. Fitted mass (M_X) for double-tags:

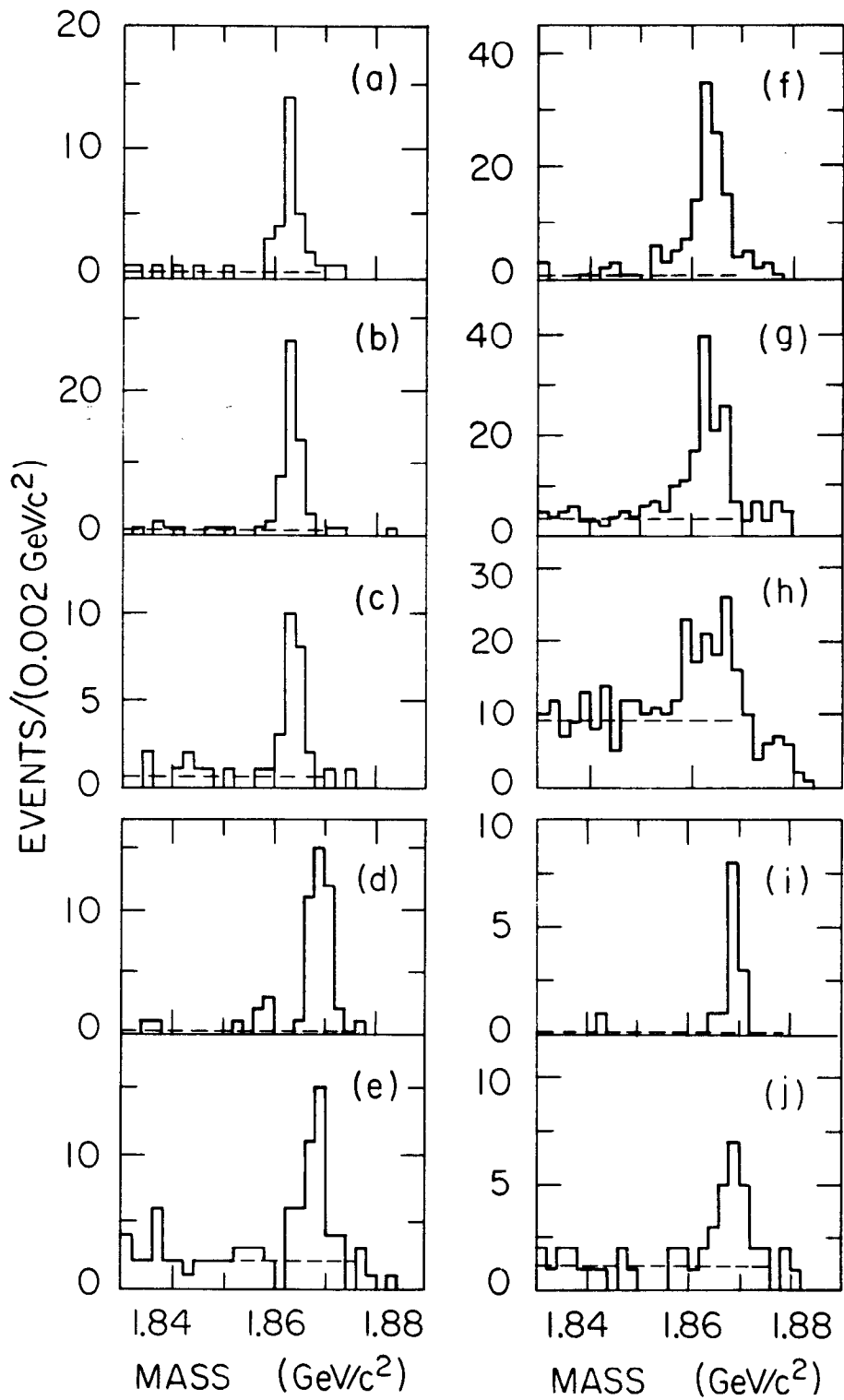
(a) $D^0\overline{D^0} \rightarrow K^-\pi^+ \text{ vs } K^+\pi^-$, (b) $D^0\overline{D^0} \rightarrow K^-\pi^+ \text{ vs } K^+\pi^+\pi^-\pi^-$, (c) $D^0\overline{D^0} \rightarrow K^-\pi^-\pi^+\pi^+ \text{ vs } K^+\pi^+\pi^-\pi^-$, (d) $D^+D^- \rightarrow K^-\pi^+\pi^+ \text{ vs } K^+\pi^-\pi^-$, (e) $D^+D^- \rightarrow K^-\pi^+\pi^+ \text{ vs } K^+\pi^-\pi^-\pi^0$, (f) $D^0\overline{D^0} \rightarrow K^-\pi^+ \text{ vs } K^+\pi^-\pi^0$, (g) $D^0\overline{D^0} \rightarrow K^-\pi^-\pi^+\pi^+ \text{ vs } K^+\pi^-\pi^0$, (h) $D^0\overline{D^0} \rightarrow K^-\pi^+\pi^0 \text{ vs } K^+\pi^-\pi^0$, (i) $D^+D^- \rightarrow K^-\pi^+\pi^+ \text{ vs } K_s^0\pi^-$, (j) $D^+D^- \rightarrow K^-\pi^+\pi^+ \text{ vs } K_s^0\pi^-\pi^0$.



1-86

5319A1

Fig. 1



1-86

5319B2

Fig. 2